ELSEVIER

Polymer 40 (1999) 5333–5344

polymer

Mechanical behaviour above T_g of a plasticised PVC reinforced with cellulose whiskers; a SANS structural study

L. Chazeau[a,*], J.Y. Cavaillé[a], P. Terech[b]

[a]*Centre de Recherche sur les Macromolécules Végétales (CNRS), Université Joseph Fourier, B.P. 53, F-38041 Grenoble cedex 9, France*
[b]*Laboratoire de Physico-Chimie Moléculaire, UMR 585, Département de Recherche Fondamentale sur la Matière Condensée, CEA-Grenoble, 17 rue des Martyrs, 38054 Grenoble cedex 9, France*

Received 11 August 1998; accepted 9 October 1998

Abstract

In previous works, the processing of nanocomposites of cellulose whisker filled thermoplastics was presented as well as their mechanical behaviour in the glassy state, both in the linear and non-linear domains. The purpose of the present work is to evaluate the mechanical properties of these composites in the rubbery state. A simple modelling of the mechanical behaviour, using the classical entropy elasticity theory, is proposed and discussed. Particular attention was paid to damage phenomena, already observed with stretched composite in the glassy state. Damage is mainly explained as a debonding of the matrix at the whisker interface. Small-Angle Neutron Scattering experiments performed on stretched composites provide supplementary information on the matrix microstructure with and without whiskers, and on the evolution of this microstructure with the sample deformation. Results confirm the heterogeneous characteristic of the matrix. Void scattering is identified and interpreted.

Keywords: Cellulose; Whiskers; Plasticised PVC

1. Introduction

New nanocomposites of a plasticised PVC matrix reinforced by cellulose whiskers were recently processed. The main characteristics of the cellulose whiskers are a high aspect ratio (about 70) and a large interface area (approximately $150\ m^2/g$). Dynamic mechanical spectrometry performed on these samples showed the interest of cellulose whiskers as they provide an interesting reinforcing effect to the thermoplastic matrix, below and peculiarly above its glass transition temperature. A mechanical model was proposed to describe the mechanical behaviour in the linear domain. Particular attention was paid to the matrix, which is assumed to be a heterogeneous medium composed of phases with different plasticiser concentration [1,2]. The description of the mechanical behaviour of both matrix and composite in the glassy state was extended to the non-linear domain. A damage process, which occurs in the composite when subjected to large deformation, was observed [3]. The specific reinforcement of the matrix in the rubbery state is caused by the presence of immobilised adsorbed chains on the whiskers surface. These chains might form a link between the whiskers and consequently create a soft whisker network [1]. A study of the mechanical behaviour of these composites in the rubbery state under large deformation was therefore desirable to establish a full description of the composite.

The first part of this article presents the result of tensile tests performed on the composites. Experimental data were analysed using the rubber elasticity theory. The damage phenomena are considered in detail and two methods are proposed to follow the damage evolution during stretching. The second part of this article is devoted to a preliminary Small-Angle Neutron Scattering study (SANS) performed on stretched matrix and composite in the rubbery state. The results provide further information on the matrix microstructure, with and without whiskers, and its evolution during the sample stretching.

2. Experimental techniques

2.1. Materials

The cellulose whiskers were obtained from a sea animal,

* Corresponding author. Groupe d'Etudes de Métallurgie Physique et Physique des Matériaux, GEMPPM,UMR INSA-CNRS, UMR 5510 F69621 Villeurbanne cedex.

E-mail address: cavaille@gemppm.insa-lyon.fr (L. Chazeau)

0032-3861/99/$ - see front matter
PII: S0032-3861(98)00748-4

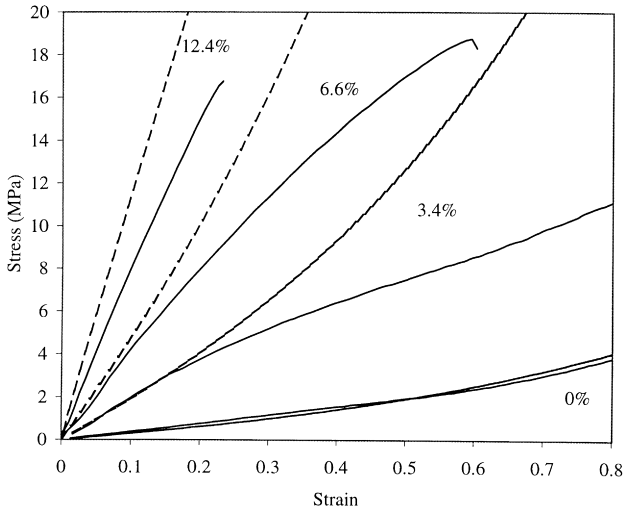

Fig. 1. Experimental true stress- true strain tensile curves (—) and theoretical curves (–-) calculated with the assumption of a rubber like behaviour (see text). Whiskers volume fraction is written on each curve. $T = 333$ K. Initial strain rate of 1.3×10^{-3} s^{-1}.

so called tunicate, after a treatment previously described [4]. The final aqueous suspension of the whiskers does not sediment nor flocculate because of electrostatic repulsion between the surface sulphate groups grafted during the sulphuric acid treatment. Poly(vinyl-chloride) (PVC) was supplied by Elf-Atochem Company (isotacticity 19%, syndiotacticity 34%; molecular weight $M_n = 40\,000$, polymolecularity index $I_p = 2$). Samples for mechanical tests were prepared as follows: the whisker suspension was blended with a PVC micro-suspension and then freeze-dried. The blend of this freeze-dried powder, 30 phr (i.e. per hundred ratio of PVC) of plasticiser (di-ethyl-hexyl phthalate fully hydrogenated) or DOP, 4.5 phr of tin-stabiliser (supplied by CIBA–GEYGY) and 1.5 phr of lubricant (stearic acid based compound), was processed by hot mixing at 180°C for 5 min. This mixture was then pressed into sheets by compression moulding at 200°C for 3 min. The composite films remain transparent.

Samples for SANS experiments were prepared following the same process. The plasticiser was provided fully hydrogenated (DOPh) or fully deuterated (DOPd). Matrices of plasticised PVC called here after pPVC, were processed with constant 30 : 100 ratio of plasticiser to PVC, but with different fractions of deuterated and hydrogenated plasticiser. Plasticised PVC was made with 0%, 40% and 100% by weight of fully deuterated plasticiser within the 30 phr of plasticiser. The corresponding samples are referred to as pPVC, pPVC/40DOPd and pPVC/DOPd, respectively. 40 wt.% of deuterated plasticiser is the calculated fraction so that the whisker scattering length density is equal to the scattering length density of the whole matrix (PVC with deuterated and hydrogenated plasticiser). Thus, it is expected that the whisker signal will be hidden by the signal of the pPVC/40DOP matrix. The scattering length density of cellulose whiskers was found equal to 18.5×10^9 cm/cm^3 (therefore, this is also the scattering length density of pPVC/40DOP).

A differential scanning calorimeter (Perkin–Elmer DSC7 system) was used to determine the glass transition temperature. The beginning temperature of the transition, T_{g1}, is 261 K, the ending temperature of the transition, T_{g4}, is 305 K. These temperatures were found to be similar for the composites, and independent of the whisker content. As a result of their small size, the whiskers appear only as bright spots under scanning electron microscopy. However, this observation indicates a good dispersion of the whiskers. The use of the electron transmission microscopy was impossible, as no sufficiently thin microtome was available. SAXS and SANS performed on the composites [5] lead to the conclusion that the dispersion of the fillers is isotropic, and without aggregates. The isotropic character of the whisker dispersion is also confirmed by comparisons and analogies with the description of whisker filled composites [6]. A study by transmission electron microscopy of whiskers extracted from the composite [5] showed that the typical length of the whiskers was not modified during the composites processing.

2.2. Tensile tests

Tensile tests were performed on a tensile mini-machine (MINIMAT RHEOMETRICS) with a temperature-controlled chamber which allows experiments between −10°C and 200°C. Experiments were conducted at 60°C with a constant crosshead speed. Initial strain rate was 1.3×10^{-3}. The samples were dumbbell-shaped (H3 norm) with typical dimensions of 17 mm efficient length, 4 mm width, and 1 mm thickness. The surfaces in contact with the clamps were specially prepared to avoid any slip. It was optically checked that deformation only took place in the thin section of the sample, and that elongation measured by the machine was only that of this section.

2.3. Neutron experiments

SANS measurements were performed on the 58 MW high flux reactor of the Laue–Langevin Institute (Grenoble, France). An incident beam wavelength λ of 6 Å was selected. The D11 spectrometer was used at three distances, 1.5, 5 and 20 m. Collimation distances were respectively 8, 5.5 and 20.5 m. The scattered beams were collected on a planar square (BF_3) multidetector with 64×64 elements (1 cm linear resolution in both dimensions) [7,8]. Absolute intensities were obtained by calibration with the standard scattering of water. SANS data reduction and usual corrections for the detector response, subtractions of the various transmissions corrected backgrounds, masking steps of the detector and absolute calibration were performed with the ILL standard programs [9]. As for elastic scattering conditions, the momentum transfer Q was defined as $Q = 4\pi/\lambda \sin\theta$, θ being half the scattering angle. Samples

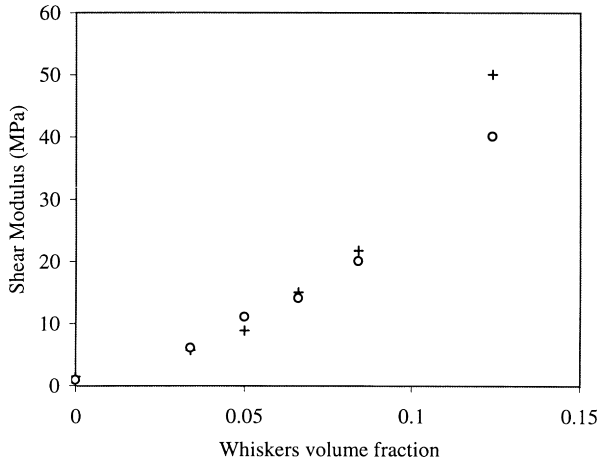

Fig. 2. Comparison between G_c measured by DMA (deduced from Ref. [1]) (+) and G_c deduced from the fit of the experimental data with the rubber elasticity theory (○).

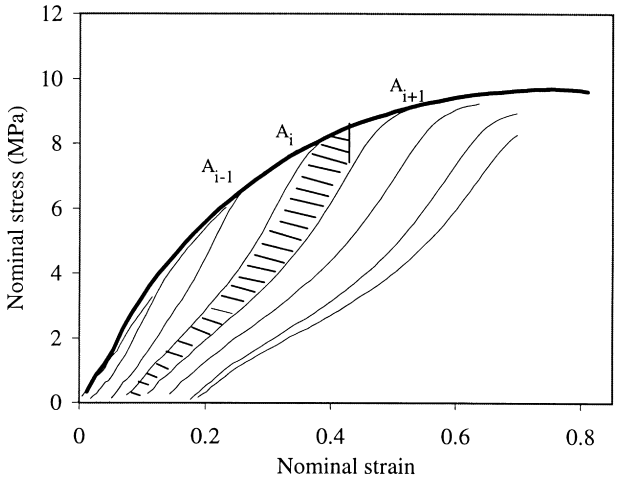

Fig. 3. Successive tensile tests performed on pPVC reinforced with 6.6 vol%. of whiskers. Stress–strain curve in bold line is obtained from a monotone tensile test. Dashed surface is assumed to be the density of the damage energy dissipated during the test A_i.

were stretched in an aluminium frame. The strain $\ln(L/L_0)$ or the stretching ratio (L/L_0) was determined from the position of small dots on the samples. Effects of biaxial deformation and of clamping were reduced by irradiating only the centre of the strips. In the case of isotropic scattering, the regrouping of the data was annular. For anisotropic signals, the cells corresponding to the same momentum transfer, Q, were regrouped inside sectors of 38° and 24° along respectively the parallel and perpendicular directions to the stretching axis.

3. Results and discussion

3.1. Mechanical behaviour

3.1.1. Tensile tests

The experimental tensile test curves are presented on Fig. 1. At 60°C, the matrix is in the rubbery state. For the deformation range studied (true strain below 0.8), the pPVC sample recovers totally its deformation when left for 1 h at room temperature. pPVC has a rubber-like behaviour because of the presence of crystallite [10], possibly enhanced by potential interaction between DOP and PVC [11], both phenomena acting as cross-links.

There is a strong increase of the elastic modulus, and more generally of the strength level with increasing whisker content. This is similar to filled elastomer behaviour, but the effects are much greater than for classical filled elastomer reinforced with the same filler fraction. This is as a result of the specific reinforcing effects of our fillers, already observed by mechanical spectrometry [1,2]. The samples showed a whitening more and more visible, appearing earlier at increasing whisker concentration. This results from damage, which finally leads to the material failure. The composite deformation was not totally recoverable even when heat-treated well above the tensile test temperature, and the non-recoverable deformation increases at increasing filler content. It highlights a probable modification of the composite microstructure during the tensile test.

The rubber-like behaviour of pPVC alone allows the use of the classical rubber elasticity theory. The simplest and most used relationship for small strain is given by:

$$\sigma = G_c(\exp(2\varepsilon) - \exp(-\varepsilon)), \quad (1)$$

where σ and ϵ are respectively the true strain and true stress, and G_c is the shear rubber modulus.

The fit of experimental curve of pure pPVC is satisfactory and supports the rubber-like behaviour analysis (cf. Fig. 1). There is an increasing divergence between theoretical curves and experimental results with increasing filler content and deformation level. It is however possible to estimate the modulus G_c of the different samples by fitting the curve for small strain. In Fig. 2, the G_c deduced from the fit is compared with the shear modulus measured by DMA at the same temperature and at frequency of 0.1 Hz[1]. There is a good agreement between the two experiments for low whisker contents. In this approach, whiskers are assumed to act as supplementary cross-links within the materials. This is supported by swelling experiments [1]. For the highest whisker concentration (12.4% by volume), the reinforcement effect measured by DMA is higher. The damage may have an impact at the very beginning of the tensile test. For DMA experiments, the imposed strain is extremely low ($<10^{-4}$), and therefore has no incidence on the material microstructure. Thus, the deviation of the experimental behaviour to the predicted behaviour might also be as a result of the damage process.

3.1.2. Damage characterisation

In the present work, damage refers to all physical processes, which modify the mechanical properties of the material. For its characterisation, successive tensile tests

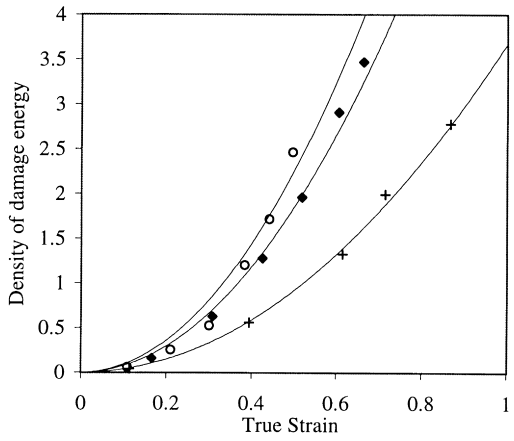

Fig. 4. Energy of "damage" (MJ/m^3), deduced from successive tensile tests performed on plasticised PVC reinforced with 3.4 vol% (+), 5 vol% (◆), 6.6 vol% (○) of whiskers ($T = 60$°C).

were performed on composites filled with 3.4 vol%, 5 vol%, and 6.6 vol% whiskers. The experiment consisted in stretching the material, under the conditions described in Section 2.1, up to a certain deformation ϵ_1 (test A_1), then releasing and putting it at 373 K (20 K above the testing temperature) for one half an hour and testing it again up to a higher deformation ϵ_2 (test A_2). This procedure is repeated with increasing deformation ϵ_i (tests A_i), until break. It is checked that half an hour is enough to attain total relaxation of the material. The unrecoverable deformation is taken into account in each successive tensile test. Pure pPVC is the only tested sample, which shows a perfect superposition of the successive stress–strain curves and a total recovery of the deformation. Fig. 3 shows the experimental results for the composite with 6.6 vol%. fillers. The stress–strain curve obtained with a monotone tensile test of the same composite is also plotted in the same figure. The observed behaviour is close to that observed for filled rubber and known in the literature as the Mullins-effect [12,13]. The composite sample stretched to a relative elongation and then released (test A_i), does not follow the same stress–strain curve when it is stretched once again (test A_{i+1}). It appears softer during test A_{i+1}, when the deformation is below the maximum deformation reached during test A_i. For further elongation, the stress–strain curve of test A_{i+1} follows the behaviour of the stress–strain curve obtained from the monotone tensile-test. Moreover, the residual strain measured after release, increases with the strain imposed during the previous tensile test. The whitening decreases during the release, and the larger the elongation of the test A_i, the earlier is the increase of the whitening during the test A_{i+1}.

The energetic approach developed by Lepie and Adicoff [14] and previously used by Heuillet [15] with filled solid propellants was also used to analyse the present data. Heuillet demonstrated that the surface bordered by two successive stress–strain curves, for tests performed as described earlier, is equal to the energy spent by the damage process during the first tensile test (cf. Fig. 3). Therefore, the cumulative energy measured by successive tests determines the damage responsible for ruin and rupture of the material. Cumulative density energy measured from these successive tensile tests is reported in Fig. 4 as a function of strain. This energy increases exponentially with the strain and more rapidly for higher whisker contents. It does not depend on the loading cycle, but only on the deformation. However, the total fracture energy is difficult to estimate from these tests or from the classic tensile tests of Fig. 2, owing to the uncertainty in the strength measurement. The fracture appears slightly earlier when the composite is submitted to successive tests. Thus, "fatigue" of the material, induced by the experiments, must lead to a slight overestimation of the measured damage energy at a given strain. This means that the energy measured can be the basis of a damage criterion only as a first approximation.

The damage is generally attributed to three phenomena: debonding at the filler-matrix interface, macromolecule rupture, and filler rupture. Multifragmentation tests performed on a unique long cellulose fibre embedded in a pPVC matrix shows that, under the same conditions as the present tensile tests, the aspect ratio of the fibre fragments obtained at the end of the test are at least three time higher than the aspect ratio of the cellulose whiskers [5]. This indicates that the whiskers, in the composites and for the testing conditions, have a length below their critical length. Fibre ruptures are therefore unlikely to occur and are not responsible for the considered damage energy. The whiskers certainly create stress concentration at their ends or between two whiskers, when the distance between them is small enough. This increases locally the matrix deformation. The plastic behaviour of pPVC below T_g^3 shows that this deformation, obtained for stress much higher than that of the tensile tests studied in this article, is recoverable, and therefore is not a consequence of macromolecule rupture. Moreover, the energy necessary to break covalent bonds is more than 10 times higher than the energy of hydrogen bonds generally at the origin of the interfacial adhesion [12,13]. Thus, the energy plotted in Fig. 4 is directly linked to the debonding at the filler-matrix interface. The latter is assumed to be irreversible, at least at the testing temperature (60°C).

The total debonding energy of the whole interface between the matrix and the fillers E_{dw} can be estimated as $E_{dw} = W_{ad}A$, where W_{ad} is the work of adhesion and A is the interfacial area per m^3 of matrix. The latter is deduced from the whisker size and their volume fraction. W_{ad} is calculated from surface energies of pPVC and cellulose measured by the angle contact technique. W_{ad} was found to be 76×10^{-3} mJ/cm^2 at 25°C [5]. Finally, for 6.6 vol% of whiskers, an estimation can be obtained: $E_{dw} = 1.7 \times 10^6$ J/m^3. Indeed, this calculation is qualitative. Surface energies are measured at equilibrium and yet it is known that the filler-matrix decohesion is a visco-elastic process. W_{ad} depends on the strain rate and the temperature [16]. However, E_{dw} is found to have the same order of magnitude as the energy density

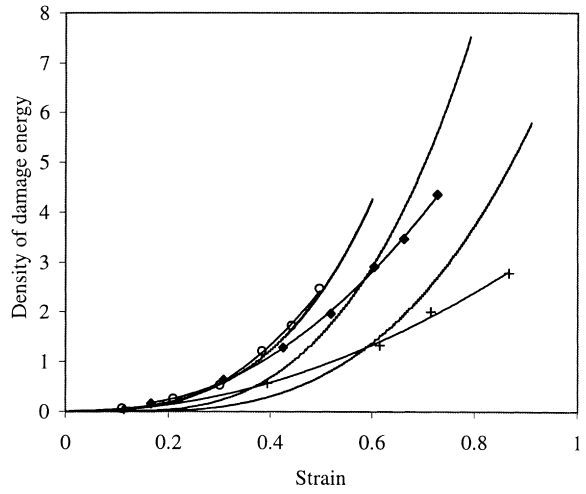

Fig. 5. Energy of "damage" (MJ/m^3), as a function of strain deduced from successive tensile tests performed on pPVC reinforced by 3.4 vol% (+), 5 vol% (◆), 6.6 vol% (○) of whiskers; comparison with energy deduced from the difference between experimental curves and curves calculated from the rubbery elasticity theory (––).

measured by successive tensile tests. This supports the hypothesis of the damage arising from a dewetting of the whiskers by the matrix.

As shown in Fig. 1, the damage energy can be estimated as the difference between the composite behaviour and the entropy elasticity theoretical prediction (based on the assumption that the whiskers act as supplementary crosslinks). Energy density, deduced from the surface between the two curves, is plotted in Fig. 5. These values are assumed to represent the theoretical damage energy density spent during tensile tests. The damage energy density, measured by multiple tensile tests, is plotted in the same figure. There is a very good agreement between these two sets of data for the composite with 6.6 vol% whisker content. The multiple test technique gives a higher value for the energy for filler fractions below 6.6 vol%, (when the stress is lower). The energy calculated from tensile tests is influenced by the non-total recovery of the deformation, especially for low stress cycle when the energy increases relatively slowly, which is the case for low whisker content. The non-recovery can be partly attributed to a friction phenomenon at the interface. It is also possible that the material reorganises its microstructure so that the local energy reaches a minimum before the total recovery of the deformation occurs.

The formation of voids, visible on reinforced samples, must also be considered. The whitening persistence after their thermal treatment, means that a certain fraction of voids do not disappear during the strain recovery. Their size might be too large to allow a total recovery of the deformation around them. Therefore, these voids make a contribution to the non-total recovery of the deformation. The void growth consumes energy during the deformation. Therefore a part of the measured damage energy results from void creation.

To summarize, the two approaches presented are convenient methods to determine the damage evolution in a material but remain questionable

(i) Firstly, it is based on the assumption currently used for filled elastomers that the composite material has a behaviour described by the rubber elasticity theory.
(ii) Secondly, it is difficult to discriminate the damage from phenomena induced by the method itself (such as fatigue or successive reorganisation of the material microstructure during each successive test).

Moreover, these tests allow to monitor the degradation of the material but do not give information on voids creation (or cavitation), although the latter is directly linked to damage and is its most obvious and visible manifestation.

3.2. Conclusion of the tensile tests

Tensile tests performed on whiskers filled pPVC show the important reinforcing effect of these fillers. The elastic entropy theory suggests that the fillers act as supplementary crosslinks inside the composite [1]. The stress–strain curve and the whitening of the samples are the manifestations of damage whose origin can be the debonding at the whisker-matrix interface. Damage can be characterised by successive tensile tests following the method developed by Heuillet. This procedure allows a "monitoring" of the damage process during the composite deformation. A certain agreement is found between the energy determined by this procedure and the energy deduced from comparison between entropy elasticity theory and experimental tensile tests. The results support the assumption of a damage, which consists of a preferential debonding of the adsorbed chains. These latter are assumed to act as supplementary crosslinking at the whisker interface. Additional experiments are required to clarify the role of the local matrix deformation and the void creation upon the mechanical properties of the composite.

In order to determine if these voids appear as soon as the macroscopic strain is applied, i.e. much before they produce visible light scattering, it is of interest to study the scattering of shorter wavelength source such as X-ray or neutron.

3.3. Neutron scattering experiments

Small angle neutron scattering (SANS) experiments were performed to observe the microstructural modification within the composites during their deformation. Owing to the complexity of our material, the signal scattered by the matrix, without whiskers, was studied first. The following two sections present and discuss the results concerning the non-stretched and stretched matrix. The third and fourth sections concern the composite.

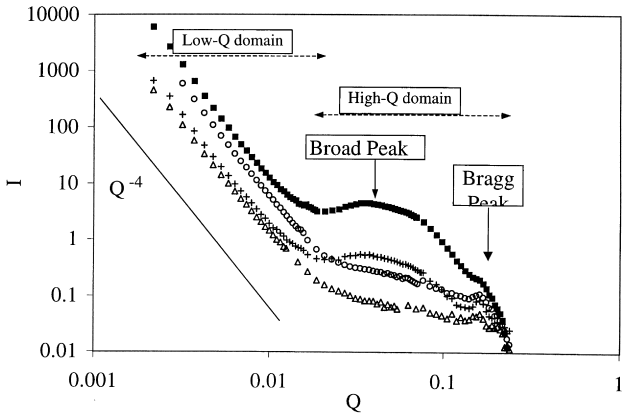

Fig. 6. Scattering curve of PVC plasticised by 30 phr of plasticiser in which 0% (i.e. pPVC) (○), 40% (PVC/40DOPd) (+) and 100% (PVC/DOPd) (■) by weight are deuterated and scattering curve of PVC (△). Q is in $Å^{-1}$ and I is in cm^{-1}.

3.3.1. Non-stretched Matrix (without whiskers)

The isointensity patterns were measured on the 2D detector of D11 for pPVC/40DOPd. The signal is isotropic. The average intensity calculated by an annular regrouping of the data is plotted as a function of Q in Fig. 6. To characterise the influence of deuterated plasticiser upon measured intensity, complementary experiments were made with PVC, pPVC, and pPVC/100DOPd. The scattering signals were checked to be isotropic for these three samples. The regrouped data as a function of Q are also displayed in Fig. 6. PVC scattering is not as flat as expected. The curve can be divided in two domains. These domains are respectively defined by a Q-range of [2×10^{-3}, 2×10^{-2} $Å^{-1}$] for the so-called "low-Q domain" and [2×10^{-2}, 2×10^{-1} $Å^{-1}$] for the so-called "high-Q domain". In the high-Q domain, the intensity decreases approximately as Q^{-1}. A Bragg peak is visible at Q between 0.14 and 0.16 $Å^{-1}$. In real space, this corresponds to a distance of periodic organisation equal to about 42 Å. It is known that fatty acids and their derivatives (molecules with long chain and carboxylic polar heads) associate as a head-to-head bimolecules, defining a distance of about 2×24 Å. Therefore, we can reasonably attribute this peak to the crystallisation of the stearic acid inside the paraffin K175, incorporated in PVC during the material processing [17]. In the low-Q domain, a large Q^{-4} intensity decrease is observed. Comparing PVC and plasticised PVC samples, pPVC does not present a scattering curve at low-Q significantly different from the scattering of pPVC/40DOPd. The same Q^{-4} decrease and the same intensity levels are observed. Conversely, plasticiser introduces a difference in the high-Q domain. A broad peak, spread over a decade, appears (cf. Fig. 6). The latter has already been considered as a scattering feature from the contrast effect between PVC ordered and disordered domains [10,18–20]. The ordered domains are usually ascribed to crystalline domains in PVC. The deuteration of a part of the plasticiser leads to an increase of intensity in the low-Q domain. However, the power law of the intensity decrease still follows a Q^{-4} function. In high-Q domain, deuterated plasticiser decreases the intensity of the broad peak, when its weight fraction represents 40 wt.%. of the whole plasticiser weight in the sample (PVC/40DOPd). When the plasticiser is fully deuterated (PVC/100DOPd sample), the broad peak is more intense, as previously observed [18]. The above observations are analysed in the following paragraph.

Table 1
Calculated scattering volumic contrast between DOP and PVC as a function of the deuterated plasticiser content in plasticiser

Samples	pPVC	PVC/40DOPd	PVC/100DOPd
Scattering volume contrast (10^9 cm/cm^3)	8.6	12	43

The coherent scattering length density of PVC is 15.7×10^9 cm/cm^3. ρ_{DOP}, the scattering length density of DOP, is a function of its deuterated plasticiser fraction, and is given by the equation: $(7.1 + 51.8x)10^9$ cm/cm^3; x is the weight fraction of DOPd. For $x = 0$, $\rho_{DOP} = 7.1 \times 10^9$ cm/cm3. The calculated volumic contrast between PVC and DOP for the different samples are reported in Table 1. The contrast between PVC and DOP is the highest when the plasticiser is fully deuterated. Contrasts calculated for pPVC and PVC/40DOPd are slightly different. The broad peak observed on the scattering curve originates from a contrast between the plasticiser and ordered PVC domains. The small difference between the volumic contrast of samples with 0 and 40 wt.%. of DOPd in plasticiser explains the small difference between the broad peak intensity of the corresponding samples. Although the calculated contrast for pPVC is slightly smaller than the contrast calculated for the PVC/40DOPd sample, the broad peak intensity is higher. This could be because of a difference of crystallinity in the material, resulting from a slightly different thermomechanical history for both samples (despite precautions to process samples under identical conditions) [18]. It is noteworthy that this remark is without consequence on the following study: indeed, the minor difference of intensity of the broad peak has no influence on the modification of the scattering signal introduced by the presence of whiskers or by the stretching of the sample (cf. later).

The scattering at low-Q of pPVC leads to a plateau in the IQ^4 vs. Q plot; such a signal is usually met for inhomogeneous biphasic systems with neat interfaces. It is noteworthy that Morrison reported the same power law intensity decrease for PVC/DOPd sample. This was found to be dependent upon the sample thermomechanical history and attributed to PVC primary particle boundaries. The microstructure of the initial particle created during PVC synthesis is known. Several authors have shown that irrespective of the machine used for the material processing, there is no

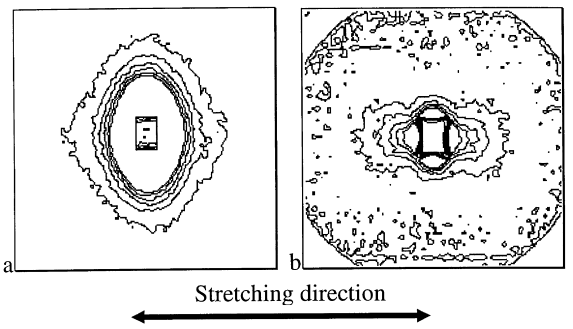

Fig. 7. Isointensity patterns at two detector distances 20 m (a) and 5 m (b) (Q domain respectively [2×10^{-3};10^{-2} Å^{-1}] and [10^{-2}; 7×10^{-2} Å^{-1}]) measured on PVC/40DOPd, stretched at a strain level $\epsilon = 0.33$ ($\lambda = 1.4$).

destruction of this microstructure for temperatures below 200°C [21]. The material is described as rigid domains in a softer medium of mobile chains. Therefore, the low-Q intensity decay measured with PVC can be explained in terms of density fluctuations created by these domains. In fact, it is likely that during the preparation procedure, a more or less thick shell of primary particles is molten, creating a medium of mobile chains. The initial microcrystallites present in the primary particles are also molten. The material is then constituted of rigid domains (made of unmolten primary particles), where the crystallites and so the physical crosslink density, are the same as before the processing, immersed in a medium made of molten polymer chains where the crosslink density is less high.

Following the Debye–Bueche random-two-phase model, the heterogeneities are assumed to be distributed according to an exponential function:

$$\gamma(r) = \exp\left(\frac{-r}{\Xi}\right), \tag{2}$$

where Ξ is a correlation length related to the average size of heterogeneities of volume fraction ϕ and r is the radial distance in the system. The corresponding scattering contribution in the Q-reciprocal space is obtained by an appropriate Fourier transform [22]:

$$I(q) = \frac{I(q)_{q\to 0}}{(1 + q^2\Xi^2)^2} \tag{3}$$

with $I(q)_{q\to 0} = 8\pi\Delta\rho^2\Xi^3\phi(1-\phi)$.

Both phases are assumed to contain plasticiser, but one is richer in DOP. The contrast $\Delta\rho$ depends upon the volume fraction of plasticiser in both phases. In the previous section, it was shown that an increase of DOPd content in plasticiser increases the DOP scattering length density; therefore, an increasing DOPd content increases the volumic contrast between the two phases and accounts for the intensity variations observed in the low-Q domain (cf. Fig.6).

The determination of the correlation length Ξ from the scattering curve is not possible as a linear fit of the square root of inverse intensity $1/I^{1/2}$ vs. Q^2 leads to a too large uncertainty in the extrapolated value $I_{Q\to 0}$. Such an analytical description has been used for polystyrene networks swelled by unlabelled mobile deuterated polystyrene chains [23]. However, the assumption of a total phase separation between DOP and PVC allows the calculation of the upper limit of the scattering particle size. In the case of PVC/40DOPd, this leads to $\Delta\rho^2 = 1.44 \times 10^{20}$ cm^{-2} (contrast between PVC and DOP in which 40 wt.% is deuterated), and $\phi = 0.71\%$. Within this assumption, a correlation length of about 1 μm is found. This is only five times larger than the estimated size of PVC particles synthesised in microsuspensions (0.2 μm). This suggests that the primary particles are possibly at the origin of the Q^{-4} intensity decrease in the low-Q domain.

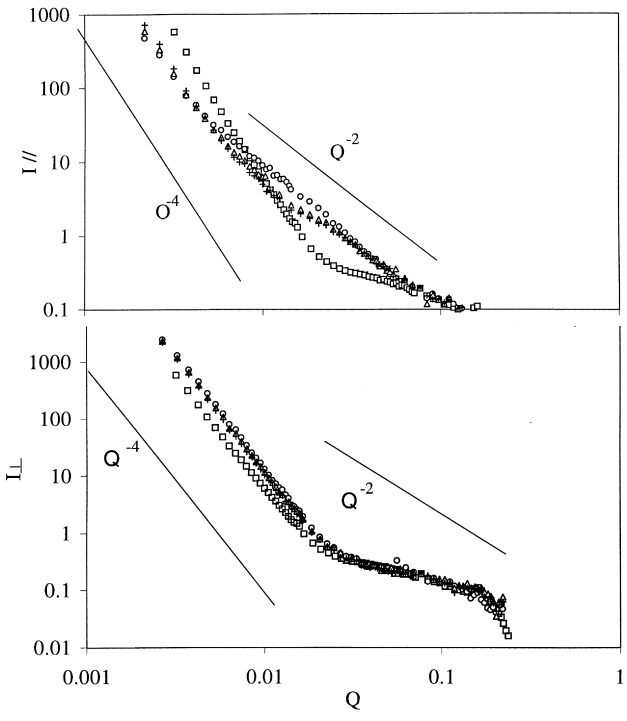

Fig. 8. Scattering intensity of PVC/40DOPd sample; $\epsilon = 0$ (□);$\epsilon = 0.33$ (+);$\epsilon = 0.4$ (△);$\epsilon = 0.5$ (○). Q is in Å^{-1} and I is in cm^{-1}: (a) $I_{/\!/}$; (b) $I_{\top}$.

3.3.2. Stretched matrix

When the PVC/40DOPd sample was stretched at different strain levels ϵ, 0.33, 0.4 and 0.5, the scattered signal becomes strongly anisotropic (Fig. 7). The isointensity patterns seems the combination of a vertical elliptical pattern, essentially observed at low-Q (Fig. 7a), and of an horizontal double-wing pattern (also called a butterfly pattern) essentially observed at intermediate Q-range (Fig. 7b), the stretching direction being horizontal.

Elliptical patterns with a principal axis in the direction orthogonal to the stretching direction are usually observed when partly deuterated adjustable mobile species are stretched. The decrease of the correlation length in the axis perpendicular to the stretching direction, and its increase in the stretching axis leads respectively to an

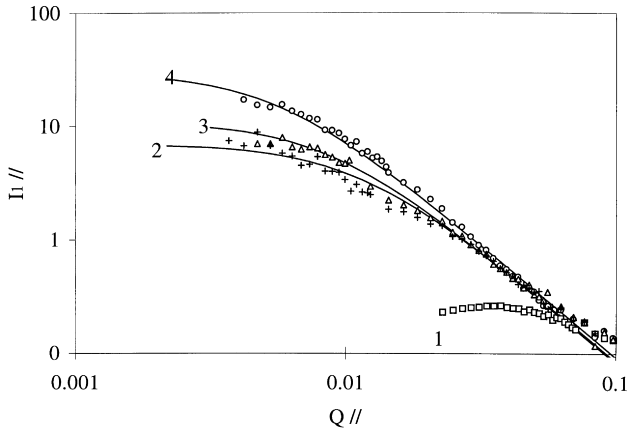

Fig. 9. Scattering of PVC/40DOPd in the stretching direction; corrected signal after subtraction of a Debye–Bueche contribution; $\epsilon = 0$ (□);$\epsilon = 0.33$ (+);$\epsilon = 0.4$ (△);$\epsilon = 0.5$ (○).

increase of the intensity in the perpendicular direction, and to a decreasing intensity in the stretching direction.

Double wing patterns are observed for stretched elastic networks in the presence of mobile species. The network can be chemically or physically crosslinked or made of entangled chains. The mobile species can be uncrosslinked linear chains or solvent molecules. Several theories have been proposed to explain this behaviour [23–26].

Fig. 8 presents the intensity along parallel and perpendicular axes with respect to the stretching direction. Two different regimes can be distinguished:

(i) In the low-Q domain, the intensity level decreases with increasing strain in the parallel direction and slightly increases in the direction perpendicular to stretching. The intensity decay follows a Q^{-4} behaviour in both directions, at any stretching ratio.
(ii) In the high-Q domain, in the stretching direction (cf. Fig. 8a), the scattering intensity increases with the stretching ratio and a Q^{-2} slope appears. Conversely, in the same Q-range, there is no significant evolution of the intensity component perpendicular to stretching direction (cf. Fig. 8b).

The intensity can be analysed as resulting from the combination of two clearly identified intensity decays $I_1(Q)$ and $I_2(Q)$. [24] $I_2(Q)$ concerns the scattering in the low-Q domain and follows the Debye–Bueche equation (cf. Eq. (3) discussed previously). $I_1(Q)$ is the deduced scattering from the subtraction of $I_2(Q)$ from the experimental scattering:

$$I_1(Q) = I(Q) - I_2(Q). \tag{4}$$

The parallel and perpendicular components of $I_1(Q)$ are different as well as those of $I_2(Q)$. $I_2(Q)$ is fitted to the experimental curves obtained in both directions (Fig. 8), in the low-Q domain. As noticed earlier, it is impossible to determine precisely I_{02}. The latter and Ξ are two adjustable parameters. Fig. 9 presents the intensity $I_{1/\!/}(Q)$ in the parallel direction, deduced by subtraction of $I_{2/\!/}(Q)$ from the experimental parallel scattering curve, for different stretching levels. The significant role played by $I_{2/\!/}(Q)$ in a large Q domain, leads to a lack of precision in the deduced $I_{1/\!/}(Q)$. For this reason, the signal deduced for the unstretched sample is difficult to analyse. It presents the same aspect as the scattering deduced for a stretched sample (cf. curve 1–4 in Fig. 9). There is a plateau at low-Q and a decrease following a Q^{-2} law at high-Q. Following Ramzi [24], this scattering can be described with a Lorentzian function:

$$I_1(Q) = \frac{I_{01}}{1 + Q^2\xi^2}. \tag{5}$$

The deduced value of $I_{01/\!/}$ and $\xi_{/\!/}$ as a function of the stretching level are reported in Table 2.

An attempt to apply the same treatment to the perpendicular intensity was inaccurate owing to the too small intensity variations for $Q > 10^{-2}$ Å^{-1}. No significant evolution of the correlation length could be deduced. It can be concluded that stretching of plasticised PVC leads to an increase of parallel correlation length and to a quasi-constant perpendicular correlation length in a Lorentzian description of the scattered intensity.

The "cluster-like heterogeneities" model [23,24,27] proposes a qualitative theoretical explanation of this behaviour. In this model, the fluctuations in the cross-link density are assumed to form a sort of superstructure, which can be discovered progressively under stretching conditions. This superstructure is made of clusters in which the cross-link density is higher than in the whole bulk sample. During stretching, the cluster-like islands are less deformed than the average. They should separate in space along the stretching direction, leading to an unscreening process in the parallel direction: the nearly exact compensation of the intra-island correlations by the inter-island correlations should progressively break down: $\xi_{/\!/}$ and $I_{01/\!/}$ should increase. The shift of $\xi_{/\!/}$ with deformation should progressively enlarge the domain $1/\xi_{/\!/} < Q_{/\!/} < 1/R$ (R is the average distance between two cross-links) and reveal the "intermediate behaviour" of the scattering. In the perpendicular direction, the reverse effect should occur: the cluster-like islands should interpenetrate; as a result, both the correlation length $\xi_\top$ and the scattering intensity $I_{01\top}$ at low-Q should decrease upon stretching at the expense of the scattering in the intermediate regime $1/\xi_\top < Q_\top < 1/R$. In the

Table 2
Values and correlation length $\xi_{/\!/}$as a function of strain, in the stretching direction, deduced from PVC/40DOPd scattering $I_{/\!/}(Q)$ corrected by subtracting the Debye–Bueche contribution $I_{02/\!/}(Q)$

Strain	$I_{01/\!/}$ (cm^{-1})	$\xi_{/\!/}$
0	(0.3)	(60)
0.33	7	90
0.44	11	115
0.51	30	180

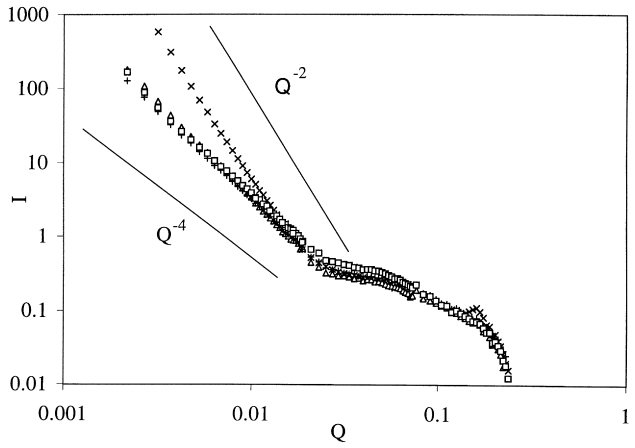

Fig. 10. Influence of the whisker content on the scattering curve of PVC/40DOPd: 0 vol% (×), 5 vol% (▯), 6.6 vol% (+), 8.4 vol% (□) of whiskers. Q is in $Å^{-1}$ and I is in cm^{-1}.

present case, as well as in the references cited earlier, the perpendicular deformation ratio ($\lambda^{-1/2}$) is much smaller than the stretching ratio λ, and so modifications of the perpendicular scattering are quite negligible.

As mentioned earlier, the butterfly patterns are observed in the high-Q range when the elliptical patterns are observed in the low-Q domain. From the discussion on the unstretched matrix scattering, it can be concluded that this elliptical pattern is created by the deformation of the biphasic structure with neat interfaces, composed of PVC primary particles more or less molten and immersed in a medium made of more mobile PVC chains. This is in agreement with the observed evolution of the signal in the low-Q domain in both direction: the Q^{-4} decrease is shifted towards low-Q in the direction parallel to the stretching axis (by a factor ϵ) and towards large Q in the perpendicular direction (by a factor $\epsilon/2$).

3.3.3. Unstretched composite

The whiskers have not been found to influence the isotropy of the scattering of the unstretched composite

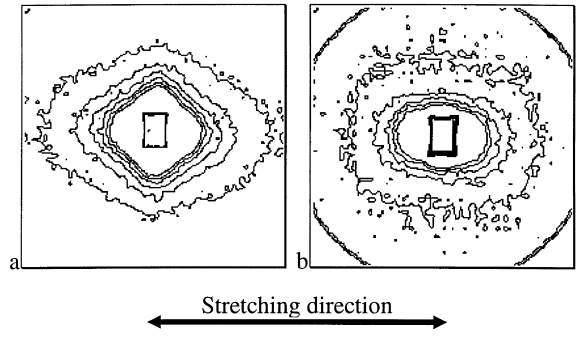

Fig. 11. Isointensity patterns at two detector distances 20 m [a] and 5 m [b] (Q domain respectively [2×10^{-3}; 10^{-2} $Å^{-1}$] and [10^{-2}; 7×10^{-2} $Å^{-1}$]), measured on PVC/40DOPd reinforced with 8.4 vol%. of whiskers, stretched at a strain level 0.33 ($\lambda = 1.4$).

materials, which means that the whisker dispersion inside the matrix is isotropic. The scattering intensity of samples with 5%, 6.6% and 8.4% by volume of whiskers is plotted in Fig. 10. In the low-Q domain, the scattering decreases following a Q^{-2} slope instead of a Q^{-4} slope observed for unreinforced samples (cf. Fig. 6). It is noteworthy that intensity values for composites in this Q region are not affected by the whisker content. In the high-Q domain, the whiskers do not modify the scattering intensity if compared to the unreinforced sample. The peak attributed to the stearic acid almost totally disappears.

It was previously noticed that PVC primary particles and stearic acid grains are still present inside the matrix after the processing and account for respectively the Q^{-4} decrease at low-Q and for the Bragg peak observed at 0.15 $Å^{-1}$ (cf. Fig. 6). The high viscosity induced by the whiskers, during the hot-mixing step of the processing, probably creates local stresses much higher than those induced inside the matrix alone, under the same processing conditions. This should lead to a better homogenisation of the material. Within this assumption, the higher the whisker content, the better the homogenisation of the composite matrix should be. During the hot-mixing step of the processing, a low whisker content is sufficient to strongly increase the pPVC viscosity. Thus the melting of the primary particles might be obtained for the less reinforced material, leading to a small influence of higher whisker concentrations on the homogeneity of the matrix. This could explain that an increase of the whisker concentration does not modify the scattering curve in the low-Q domain.

In the intermediate Q-range, an increasing whisker content leads to a slight increase in the intensity. Whiskers suspensions in D_2O as well as in plasticised PVC have been studied [5]. Their scattering curve is that of isolated and infinite length parallelepipeds [28]. Thus, they present all corresponding form-factor scattering features: a Q^{-1} slope at low-Q, a Q^{-2} slope in the Guinier region (10^{-2} $Å^{-1}$ < $Q < 4 \times 10^{-2}$ $Å^{-1}$) and a Q^{-4} slope at large Q (Porod law). Although the deuterated plasticiser fraction in the matrix was calculated so that the scattering length density of the whiskers be equal to that of the matrix (cf. Section 2), the contrast between the matrix and the whiskers might not be strictly null. Therefore, the increase of the whisker content might lead to a small increase in the scattering intensity in the Guinier region. The interpretation of the $Q^{-2.3}$ slope at low-Q induced by the whisker presence is difficult. It is possible that the $Q^{-2.3}$ intensity decrease was hidden in the unreinforced sample by the Q^{-4} scattering decrease. The improved mixing of the material during processing might lead to an increase of the correlation length of the density fluctuation discussed previously: the cluster heterogeneities because of DOP concentration fluctuation might have a larger size, leading to a shift of the Q^{-2} slope towards lower Q. However, this assumption is still questionable because it does not explain the signal evolution in the [10^{-2} $Å^{-1}$;6×10^{-2} $Å^{-1}$] Q-range.

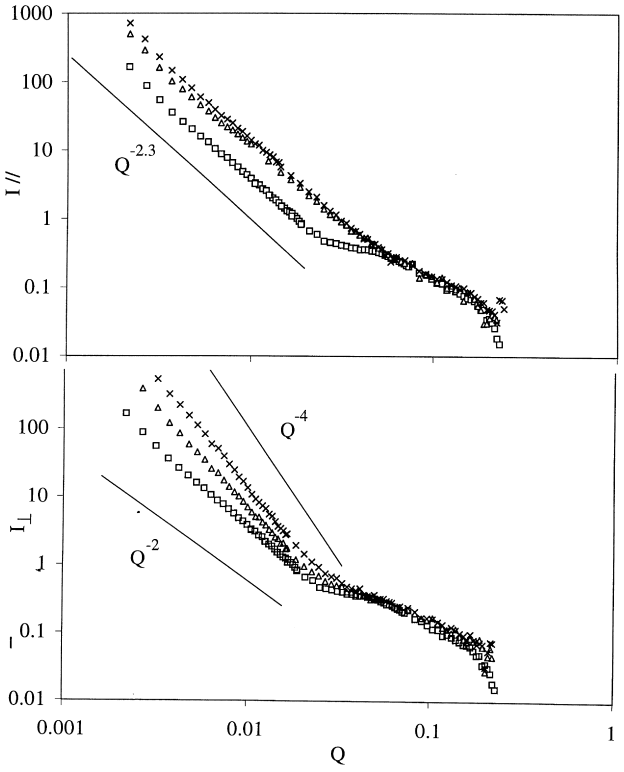

Fig. 12. Scattering curve of PVC/40DOPd reinforced with 8.4 vol% of whiskers: (a) in the stretching direction; (b) in the perpendicular direction to the stretching. Q is in $Å^{-1}$; $I_{//}$ and $I_{\perp}$ are in cm^{-1}. $\epsilon = 0$ (□); $\epsilon = 0.34$ (△); $\epsilon = 0.41$ (×).

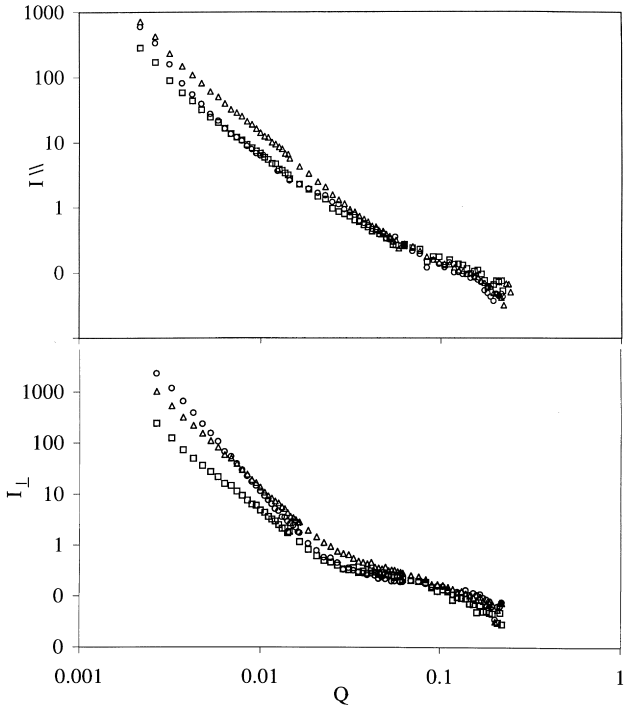

Fig. 13. Influence of the whiskers content on the scattering curve of pPVC/40DOPd at a given strain level $\epsilon = 0.4$: (a) in the stretching direction; (b) in the perpendicular direction to the stretching. Q is in $Å^{-1}$; $I_{//}$ and $I_{\perp}$ are in cm^{-1}. 0 vol% (○), 5 vol% (□), 8.4 vol% (△) of whiskers.

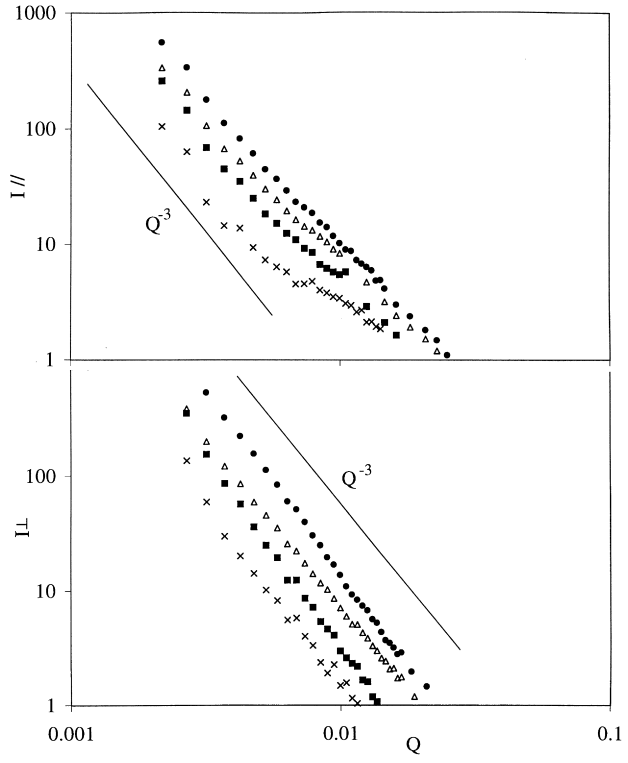

Fig. 14. Intensity (a): $I_{//}$ (stretching direction) and (b): $I_{\perp}$ (perpendicular to stretching) deduced from subtracting the scattering of the unstretched composite from the scattering of the stretched composite, for (i) samples reinforced with 5 vol%. of whiskers: $\epsilon = 0.4$ (×) and $\epsilon = 0.5$ (■) and (ii) samples reinforced with 8.4 vol% of whiskers: $\epsilon = 0.4$ (△) and $\epsilon = 0.5$(●). Q is in $Å^{-1}$; $I_{//}$ and $I_{\perp}$ are in cm^{-1}.

3.3.4. Stretched composite

Neutron scattering spectra were collected for stretched composites (cf. Fig. 11). For the same deformation level, the 2D isointensity patterns strongly differ from those of the matrix alone (cf. Fig. 7). The elliptical patterns and the butterfly patterns are difficult to distinguish. The average scattering along the parallel and perpendicular axes measured for a sample with 8.4 vol%. whisker content is plotted in Figs. 12a and 12b, respectively.

In the parallel direction (cf. Fig. 12a), the stretching seems to induce the same scattering intensity evolution as that first observed with the stretched unreinforced matrix and attributed to cluster heterogenities. However, this phenomenon is difficult to distinguish from the strong intensity decrease ($I \propto^{-2.3}$) in the low-Q domain, which extend towards higher Q with an increased stretching ratio. In the perpendicular direction (cf. Fig. 12b), in the low-Q domain, an increase of the slope with an increase of the stretching ratio is observed. Before discussing these results, the influence of the whiskers on the scattering of the composite at a given stretching ratio is shown in Fig. 13. The influence of stretching is more pronounced at a given strain level when increasing the whisker content. Thus, a phenomenon occurs in the composite, which does not occur in the unreinforced matrix. It is noteworthy that the intensity, measured at fixed

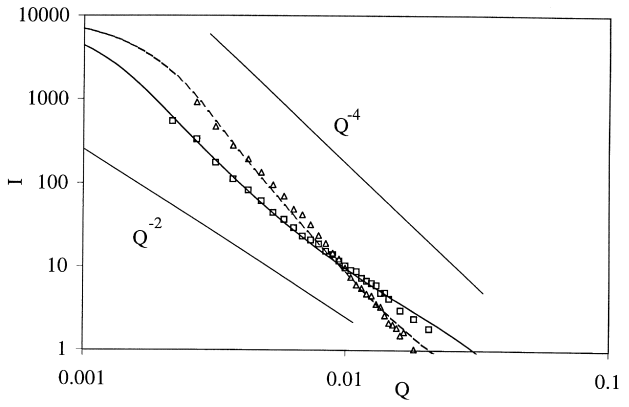

Fig. 15. Scattering intensity deduced from subtracting the scattering of the unstretched composite to the scattering of the stretched composite, for PVC/40DOPd sample reinforced by 8.4 vol% whiskers, in the stretching direction (◆) and in the perpendicular to stretching direction (Δ);$\epsilon = 0.4$. Theoretical scattering curves for spheres: (i) $R_0 = 2000$ Å; $B = 29$; $k = 10000$ (—) and (ii) $R_0 = 2000$ Å; $B = 29$; $k = 10\ 000$ (--). Q is in Å^{-1} and I is in cm^{-1}.

whisker content increases in both directions with the stretching ratio, conversely to the observations made for the matrix alone. The whitening observed during tensile tests suggests the presence of microvoids induced by stretching. Therefore, it is possible that the scattering at low-Q might contain a component from these microvoids. Within this assumption, a subtraction of the intensity scattered by an unstretched composite from the scattering of the same stretched composite, should provide the scattering from these voids. Fig. 14 presents the deduced scattering intensities in both directions. In the perpendicular direction, the deduced scattering at low-Q decreases following $Q^{-3.1}$ (cf. Fig. 14a). In the parallel direction, a $Q^{-2.5}$–Q^{-3} decrease is observed (cf. Fig. 14b). In both directions, there is the same dependence of the intensity level upon the whisker content or the strain level. This supports the idea that this scattering at low-Q is caused by void creation, as this is one of the

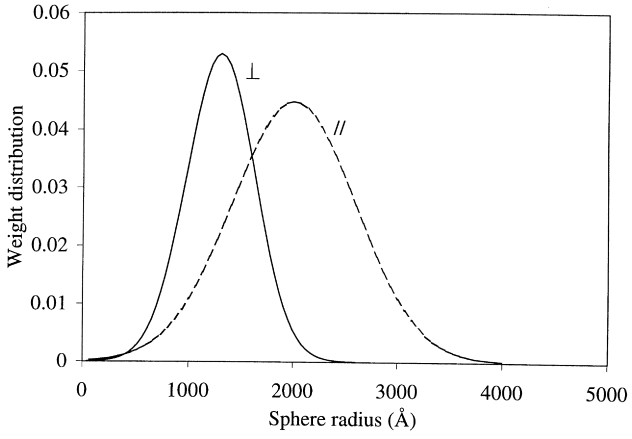

Fig. 16. Distribution of sphere radius calculated from the fit of curves in Fig. 15.

phenomena which can lead to an intensity increase in both directions. Fig. 15 shows that the parallel and perpendicular scattering are not superimposable. These results suggest the existence of an anisotropic distribution of spherical or ellipsoidal voids whose interspherical distance is larger in one direction than in the other. The theoretical form factor $P(q)$ of spheres is given by the equation:

$$P(Q) = \frac{9}{(Qr)^3}(\sin(Qr) - Qr\cos(Qr))^2, \quad (6)$$

where r is the sphere radius. The scattering intensity is proportional to $P(Q)$, with a factor k which depends upon the sphere concentration and the scattering volume contrast ($I(Q) = k \times P(Q)$). For sake of simplicity, the contribution, in the intensity, of the structure factor of spheres is neglected. For a large sphere concentration, this would lead to the appearance of a correlation peak on the scattering curve [29]. This is not observed in the present case. Fig. 15 presents the fit of Eq. (6) to the scattering curve of a composite reinforced with 8.4 vol% whiskers, in both directions. A Gaussian distribution (width B) of the sphere radius around the average value R_0 is introduced. It makes the oscillation of the theoretical scattering intensity disappear, and modifies the slope at a given Q. The parameters of the fit are therefore B, k and R_0. The deduced radius distributions are plotted in Fig. 16 for both directions. It is found to be 2000 and 1300 Å respectively for the stretching direction and the direction perpendicular to stretching axis. It is noteworthy that the same factor k is used, i.e. a priori the same void concentration. The radius average value is higher in the stretching direction which is consistent with the fact that during stretching, the spherical voids move apart in the parallel direction and draw nearer in the perpendicular direction (ellipsoidal voids can also be formed). Fig. 14 shows that an increasing whisker content or an increasing stretching ratio leads to a scattering in the low-Q domain which only differs in its intensity. This means, as expected within the hypothesis of scattering by voids, that an increasing stretching ratio leads to an increasing void concentration.

3.4. Conclusion of the SANS study

This section presents a preliminary SANS study on plasticised PVC reinforced by cellulose whiskers above its glass transition. The SANS technique was chosen as a new characterisation technique of the whiskers in suspension and to determine the quality of their dispersion in the composite. This issue has been previously presented [5] and will be the topic of a future publication. SANS experiments were also an opportunity to gain information on the matrix itself, its microstructure, and its behaviour during stretching, all information of paramount importance to understand the composite mechanical behaviour. The matrix heterogeneity was pointed out, especially the presence of primary particles and plasticiser concentration fluctuation in the matrix. A

treatment based on recent work [24] allows the definition of the correlation length of cluster-like heterogeneity whose origin is the microcrystallite (or ordered domain) density fluctuation in PVC. The stretching of the matrix leads to the appearance of butterfly patterns because of the anisotropic unscreening of the more cross-linked (ordered) cluster. These results confirm the validity of a modelling of the material mechanical behaviour, which considers it as an heterogeneous medium resulting from gradient of plasticiser concentration [2,3]. The scattering intensity and therefore the microstructure of which it is the signature, depends on the thermomechanical history of the materials. This is mainly the case for the scattering at low-Q which is, in the matrix, because of the presence of partially molten primary PVC particles. These particles are not present in the composite because the stresses induced during the material processing allow a better homogenisation. The matrix deformation process seems to be basically similar with or without presence of the whiskers, as suggested by the scattering of the stretched matrix and composite, in the high-Q domain. The main modification introduced by the whiskers is the presence of voids, revealed by the whitening of the composite samples under high stretching. It is likely that the low-Q SANS scattering of these samples includes the signature of voids whose radii (or the distances which separate them) are certainly widely dispersed. The present work shows that it is possible to follow the evolution of their characteristic distances during stretching. However, it is still difficult to have a quantitative description of their growth and deformation considering the complexity of the matrix scattering pattern.

4. Conclusion

Tensile tests showed the interesting mechanical properties of the composite above T_g. These results confirm previous work which exhibited the strong increase of the composite modulus with whisker content. The composite has a behaviour of filled elastomer. It can be modelled in a first approximation with the help of the rubber elasticity theory and it is assumed that the discrepancy between theory and experimental values is because of the damage phenomena. This damage can be characterised by successive tensile tests. It mainly consists of a dewetting of the whiskers by the matrix. The voids, revealed by a whitening of the sample, are likely to grow from the interface. SANS experiments investigated the microstructure of the matrix with and without whisker. The heterogeneous characteristic of the matrix is confirmed. Moreover, scattering of stretched composite can be partly interpreted as resulting on the basis of microvoids formation during the deformation process.

Acknowledgements

The authors would like to thank Elf-Atochem society, the ADEME and the Ecotech program for their financial support. They also thank the Laue–Langevin Institute for providing the neutron beams, and the local contacts P. Lindner and B. Demé for their help. They are particularly indebted to J.F. Legrand and R. Borsali for stimulating discussions. W. Pickout–Hintzen is acknowledged for providing the stretching machine for neutron experiments.

References

[1] Chazeau L, Cavaillé JY, Dendievel R, Boutherin B. J Appl Polym Sci, in press.
[2] Chazeau L, Cavaillé JY, Paillet M. J Polym Sci Polym Phys, submitted.
[3] Chazeau L, Cavaillé JY, Perez J. J Polym Sci Polym Phys, submitted.
[4] Sassi JF. Ph.D. Thesis, Joseph Fourier University of Grenoble, 1995.
[5] Chazeau L. Ph.D. Thesis, Joseph Fourier University of Grenoble, 1998.
[6] Hajji P, Cavaillé JY, Favier V, Gauthier C, Vigier G. Polymer Composites 1996;17:612.
[7] Ibel K. J Appl Crystallography 1976;9:296.
[8] Lindner P, May RP, Timmins PA. Physica B 1996;180/181:967.
[9] ILL. ILL Guide to the neutron research, Grenoble, France, 1998.
[10] Ballard DGH, Burgess AN, Dekoninck JM, Roberts EA. Polymer 1987;28:3.
[11] Mutin PH, Guenet JM. Macromolecules 1989;22:843.
[12] Bueche F. J Appl Polym Sci 1960;IV(10):107.
[13] Bueche F. J Appl Polym Sci 1961;V(15):271.
[14] Lepie AH, Adicoff A. J Appl Polym Sci 1974;18:2165.
[15] Heuillet P. Ph.D. Thesis, University of Compiëgne, 1992.
[16] Gent AN, Schultz J. J Adhesion 1972;3:281.
[17] Terech P, Rodriguez V, Barnes JD, McKenna GB. Langmuir 1994;10:3406.
[18] Morrison JD, Burgess AN, Stephenson RC. Polymer 1994;35(11):2272.
[19] Blundell DJ. Polymer 1979;20:934.
[20] Theodorou M, Jasse B. J Polym Sci, Polym Phys 1986;24:2643.
[21] Cogswell FN. Pure Applied Chem 1983;55(1):177.
[22] Debye P, Anderson Jr. HR, Brumberger J. J Appl Phys 1957;28:679.
[23] Ramzi A, Hakiki A, Bastide J, Bouè F. Macromolecules 1997;30:2963.
[24] Ramzi A, Zielinski F, Bastide J, Bouè F. Macromolecules 1995;28:3570.
[25] Bastide J, Leibler L, Prost J. Macromolecules 1990;23:1821.
[26] Onuki A. J Phys II 1992;2:1505.
[27] Bastide J, Mendes E, Boué F, Buzier M, Lindner P. Makromol Chem, Macromol Symp 1990;40:81.
[28] Mittelbach P, Porod G. J Acta Phys Austriaca 1961;14:185.
[29] Hayter JB, Penfold J. Molecular Physics 1981;42:109.